June 1978

Calculated Yields and Slowing-down Spectra for Electrons in Liquid Water: Implications for Electron and Photon RBE

R. N. Hamm
Oak Ridge National Laboratory

H. A. Wright
Oak Ridge National Laboratory

Robert Katz
University of Nebraska-Lincoln, rkatz2@unl.edu

J. E. Turner
Oak Ridge National Laboratory

R. H. Ritchie
Oak Ridge National Laboratory

PHYS. MED. BIOL., 1978, Vol. 23, No. 6, 1149–1161. Printed in Great Britain

Calculated Yields and Slowing-down Spectra for Electrons in Liquid Water: Implications for Electron and Photon RBE

R. N. HAMM, PH.D.,† H. A. WRIGHT, PH.D.,†
ROBERT KATZ, PH.D.,‡ J. E. TURNER, PH.D.† and
R. H. RITCHIE, PH.D.†

† Health and Safety Research Division,
Oak Ridge National Laboratory, Oak Ridge, TN 37830, U.S.A.

‡ Department of Physics, University of Nebraska,
Lincoln, NB 68588, U.S.A.

Received 4 *December* 1977, *in final form* 24 *March* 1978

ABSTRACT. Detailed Monte Carlo calculations have been carried out of slowing-down spectra and yields for a number of end-points for electrons in liquid water. These investigations were made to study differences in physical effects of different low-LET radiations and implications for RBE. Initial electron energies from 1 keV to 1 MeV were used, and all secondary electrons were followed in the computations until their energies fell below 10 eV. Though there are substantial differences in the slowing-down spectra at energies near and above the K-shell ionisation potential of oxygen, the energy spectrum of electrons at lower energies is found to be essentially independent of the initial energy of the primary electron. The number of events per unit energy deposited is also essentially independent of the primary electron energy. Based on these calculations, there appears to be little basis for ascribing differences in RBE for low-LET radiations to differences in physical effects produced by secondary electrons of low energy ($\lesssim 1$ keV).

1. Physical and biological response to low-LET radiations

The response of various detectors to low-LET radiations of different types (e.g. electrons and photons of different initial energy spectra) has been widely studied with diverse and sometimes contradictory results. In this section we review briefly the experimental evidence for a number of physical and biological systems. Differences in response between X-rays and gamma rays which are routinely noted in biological investigations seem to be relatively infrequent in physical investigations.

In many detectors the dose–response function is linear at low dose and saturates exponentially at high dose. The response is a single-valued function of the absorbed dose, as for alanine (Bermann, de Choudens and Descours 1971), dye-cyanide (McLaughlin, Rosenstein and Levine 1975, Attix 1977, private communication) and photographic emulsion (Greening 1951) for photon and electron energies from about 25 keV to a few MeV. Even when the dose–response curve for emulsions is supralinear (Katz, Larsson, Pinkerton and Benton 1977), its shape is independent of the energy. This result has been found for electron beams from 70 to 1200 keV (Dudley 1951) and for X-rays from 30 to 150 kV_p (Katz and Pennington 1978).

0031-9155/78/0006-1149 $02.00

The sensitivity of the Fricke dosemeter increases with increasing photon or electron energy from $G = 13$ to 15·5 ions per 100 eV as the incident energy increases from 10 keV to 10 MeV (Law and Redpath 1968, Law 1969, Shalek and Smith 1969, Law and Naylor 1971, 1972). Due to uncertainties in the data, the possibility is not excluded that the response is the same for both photons and electrons above 100 keV and is energy independent there.

The LiF thermoluminescent dosemeter is found to respond equally to absorbed dose from 20 to 50 kV_p X-rays and from ^{60}Co gamma rays (Law 1973), though there is some experimental disagreement about the uniformity of response to electrons above 1 MeV (Paliwal and Almond 1975).

Some explanations of the variation of effectiveness with different radiations and from detector to detector hinge on the size of the sensitive elements (Kellerer and Rossi 1972). Sensitive elements are sometimes rather clearly identified, as in the silver halide crystal of a photographic emulsion, and sometimes rather obscure, as in a scintillation counter, a Fricke dosemeter and even a biological cell. Limits can sometimes be set on possible interactions between neighbouring ionising events by ascribing a size to a sensitive element or by energy or radical diffusion lengths. Any comparison of the relative effectiveness of different radiations in different detectors must include a comparison of their sensitive element sizes. It is something of a puzzle that the Fricke dosemeter displays a decline in relative response as the energy of the incident low-LET radiation decreases, while other detectors having the same radiosensitivity and the same 'sensitive element sizes' do not.

The range in 'sensitive element size' in these detectors is quite large. In alanine and dye-cyanide the response is from the interaction of electrons with single molecules, so that the sensitive element size is of the order of 10 Å. There is not a well defined sensitive element for either the Fricke dosemeter or for LiF, though this has been treated as a fitted parameter in track theory (Katz, Sharma and Homayoonfar 1972) with a value of 50 Å. Radiation chemists speak of radical–radical interactions over distances up to 50 Å in aqueous chemistry (Draganic and Draganic 1971). The grain diameter of emulsions varies from 0·1 to 2 μm. Since the density of silver bromide is 6·5 g cm^{-3}, the equivalent 'diameter' of the emulsion grain (in water) is from 0·6 to 13 μm. In biological cells, estimates of the size of the sensitive targets vary from 0·1 to 5 μm. From the 'granularity' of energy deposition, we might expect the size of a hypothetical sensitive element that acts collectively to the transit of an electron to play a role in the response to different low-LET radiations. In many cases the total energy of a photon might be deposited in a large sensitive element, while only a single ionisation might take place in a small one.

It is convenient to describe the behaviour of detectors through the use of target theory (Dertinger and Jung 1970), making use of models which have been called multi-hit and multi-target detectors. It is assumed that there are sensitive elements (emulsion grains, or elements within the nucleus of a biological cell) which may require single hits, or many hits in a single target, or single hits in several targets in the same sensitive volume, in order to produce

the observed end-point. Physically, a hit is interpreted as a registered event caused by an electron passing through the sensitive site, with an efficiency which depends on the electron's speed. A 1-hit detector is one in which it is assumed that there is a single target in which one hit can lead to the end-point. From Poisson statistics, such a detector displays an exponentially saturating response with dose of the form $1-\exp(-D/D_{37})$, where D is the absorbed dose and D_{37} is the dose for $1/e$ survival, characteristic of the radiation. For such a detector, track theory shows that the dose–response curve always has the same shape, whatever the radiation. Here it is the numerical value of the D_{37} dose which changes. Such systems as alanine, the dye-cyanide dosemeter, most photographic emulsions, the Fricke dosemeter, many thermoluminescent dosemeters, enzymes and viruses all display 1-hit response to ionising radiations.

With many-hit detectors (specially processed photographic emulsions, and possibly the supralinear traps of TLD's; Katz *et al.* 1977) a single electron passing through a grain is unlikely to result in an observable event. There is an accumulation of damage from several electrons before the detector can yield a signal. If the energy deposition is sufficiently large in the sensitive element from a single photon, we might expect the shape of the dose–response curve to change with the type of radiation in grains of large enough size. This change has been sought by Dudley (1951) and by Katz and Pennington (1978) in supralinear emulsions (because biological systems are frequently supralinear), but has not been observed.

In sum, we see no clear change either in the shape of the dose–response curve or in the sensitivity of physical detectors to different low-LET radiations for incident energies above 100 keV in any of the preceding detectors. With the Fricke dosemeter, low-energy (10 keV) X-rays are less effective than gamma rays by about 15 to 20%.

The biological results are quite different. At energies above 1 MeV there seems to be agreement that photons and electrons produce biologically equivalent results (Wambersie, Dutreix, Dutreix, Lullouch, Moustacchi and Tubiana 1966, Wambersie and Dutreix 1971). There also seems to be general agreement that the RBE of ^{60}Co gamma rays relative to orthovoltage (250 kV_p) X-rays is about $0{\cdot}85 \pm 0{\cdot}15$ for doses of about 200 rad (Sinclair and Kohn 1964). Values of the RBE as low as 0·6 have been reported (Hendry 1972). Additionally, it is noted that the RBE decreases at low dose (Schmid, Rimpl and Bauchinger 1974) down to 0·5 at 100 rad for chromosome aberrations and down to 0·6 at 10 rad for pink somatic mutations in *Tradescantia* (Underbrink, Kellerer, Mills and Sparrow 1976). It is further suggested on microdosimetric grounds (Bond, Meinhold and Rossi 1977) that the effectiveness of ^{60}Co gamma rays might fall as low as 0·25 with respect to 250 kV_p X-rays at low dose. The observations and inferences from the biological detectors seem at odds with the observations made on physical detectors having similar dose–response characteristics and similar 'sensitive element sizes'. Clearly, this apparent inconsistency needs further elaboration and clarification.

Explanations for the variation in biological response with different low-LET radiations are often made at the 'physical' level of the interactions. One

deals with the number of ionisations produced by electrons of different energies and with the difference in the fraction of the dose occurring near the end of a track. To address the relevant physics, we have initiated a series of detailed Monte Carlo calculations of the transport of a primary electron and all of its secondaries in liquid water. Primary electron energies from 1 keV to 1 MeV were used, and secondary electrons were followed until their energies dropped below 10 eV. We calculated the electron slowing-down spectra and the yield of a number of different ionised species, of excited species and of low-energy electrons (track ends) from source electrons of energy from 1 keV to 1 MeV.

2. Calculation of electron transport through liquid water

Calculations of the slowing down of electrons in a liquid are often based on cross-sectional data obtained from the gas phase. Such computations ignore collective effects, in which a large number of electrons ($\sim 10^9$) in the condensed phase interact coherently with a passing electron. Collective states, such as the plasmon, are excited abundantly by electrons with energies below 100 eV. Therefore, they can be expected to play a role in determining the responses of physical and biological detectors discussed in the last section. An appropriate parameter to use in place of the usual macroscopic cross-section is the inverse mean free path (IMFP) for the condensed medium, which *a priori* includes all collective electron interactions.

We have constructed IMFPs for inelastic events in liquid water based on measurements by Heller, Hamm, Birkhoff and Painter (1974) of the energy dependence of the dielectric response function for liquid water up to 26 eV and on data for the isolated water molecule. The dielectric response function was fitted to the observed optical data at zero momentum transfer and constrained to exhibit the correct asymptotic behaviour in passing into the Bethe ridge for large energy and momentum transfers. In addition, the dielectric function satisfies the Bethe sum rule for all values of the momentum transfer. The IMFPs are further refined into partial IMFPs for 21 separate events, such as ionisation, excitation and radical formation. Collective effects are included through the employment of the dielectric function. The specific details that go into the determination of the IMFPs (including the differential values) for inelastic and elastic events are given elsewhere (Hamm, Wright, Ritchie, Turner and Turner 1975). The total elastic and inelastic IMFPs for electrons in liquid water are shown in fig. 1. The transport elastic IMFP is obtained by weighting the differential elastic IMFP by the factor $1-\cos\theta$, where θ is the scattering angle. The transport IMFP gives a qualitative measure of the importance of elastic scattering in electron penetration. The calculations include special relativity and exchange and presently cover electron energies up to 1 MeV. The inelastic differential IMFPs give values of the stopping power of water for electrons that agree down to several hundred eV with those given in ICRU (1970). Differences at lower energies are of the order of uncertainties in knowledge of the stopping power there.

The IMFPs have been used in a Monte Carlo program for calculating the transport of electrons through liquid water (Hamm *et al.* 1975). The program gives a detailed accounting of all individual events that a primary electron and all of its secondaries experience in slowing down to an arbitrary low-energy cut-off, taken here to be 10 eV. The overall validity of the Monte

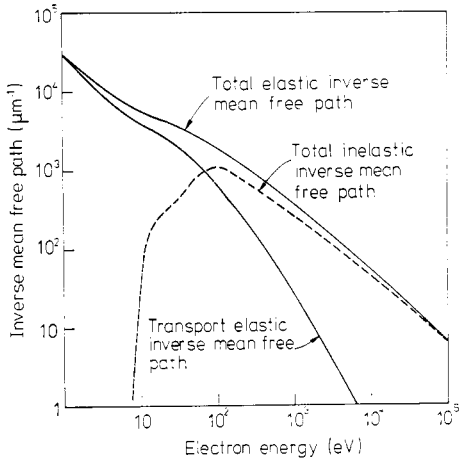

Fig. 1. Elastic and inelastic inverse mean free paths (per micrometre) in liquid water as functions of electron energy. The transport inverse mean free path is obtained from the elastic by weighting with the factor $1-\cos\theta$, where θ is the scattering angle.

Carlo transport program can be inferred from the energy dissipation curves in fig. 2. The curves show the energy deposited per micrometre of depth in a liquid water target bombarded with a broad beam of 100 keV electrons. The solid curve rests on a large body of experimental data parameterised for different condensed materials by Kobetich and Katz (1969) and applied to water. The points show results calculated for 500 electrons with the present program, the dashed curve being drawn to show the trend of the points.

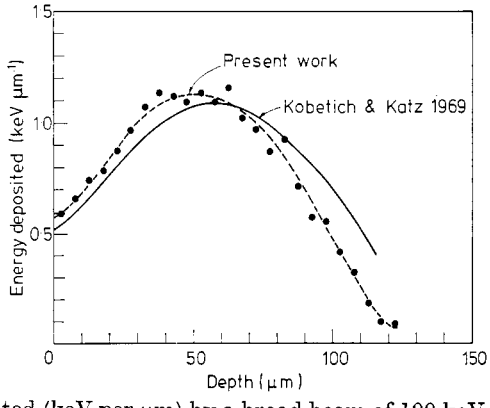

Fig. 2. Energy deposited (keV per μm) by a broad beam of 100 keV electrons as a function of depth of penetration in liquid water. Solid curve shows determination from Kobetich–Katz parameterised experimental data on a number of materials applied to liquid water. Points were calculated with the present Monte Carlo program for 500 primary electrons. Dashed curve shows general trend of calculated data.

3. Calculated slowing-down spectra and event yields

Calculated electron slowing-down spectra from monoenergetic electrons of initial energy from 1 keV to 1 MeV in liquid water are shown in fig. 3. The normalised pathlengths, in cm eV^{-1} per eV of initial energy, are shown as functions of the energy from 10 eV to 1 MeV. The curves jog at the K-shell ionisation potential of oxygen (532 eV), because of Auger electron emission.

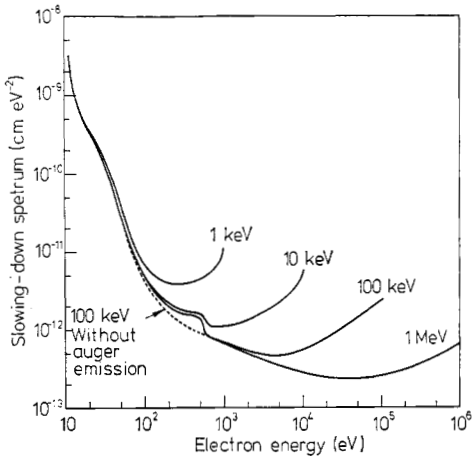

Fig. 3. Electron slowing-down spectra in liquid water for electrons of initial energy 1 keV, 10 keV, 100 keV and 1 MeV.

One sees a bulge in the region 20 to 30 eV arising from collective effects in liquid water. It is most significant for present purposes that the curves for 1 MeV and 100 keV electrons merge below 1 keV and that the curves for 100 keV and 10 keV electrons merge below 100 eV. The slowing-down spectra thus appear to be independent of the primary electron energy after about two decades of energy degradation. There are, of course, large differences at high energies.

We also calculated the slowing-down spectrum for 100 keV electrons under the condition that no Auger electrons are emitted. The results are shown by the dashed line under the Auger jog in fig. 3. They seem consistent with the suggestion of Fano and Spencer (1975) that Auger electrons be included as a source term in the continuous slowing-down calculations of the degradation spectrum.

Slowing-down spectra give only indirect information of the spatial correlation between energy-transfer events. Is it more likely with one primary energy than another, say, that ionisations from a single electron occur in two strands of DNA? An indication of similarities in spatial correlations can be found from the number spectrum of electrons produced at different energies in the degradation process. Such spectra for 1 MeV, 100 keV and 10 keV initial

energy are shown in fig. 4; the corresponding kinetic energy spectra are shown in fig. 5. In both figures the abscissa is broken into three scales, for convenience in plotting and for the accumulation of statistics: from 0 to 100 eV in 5 eV intervals, from 100 to 500 eV in 50 eV intervals and from 500 to 3000 eV in 500 eV intervals. The data are plotted on a per-incident-electron basis. In

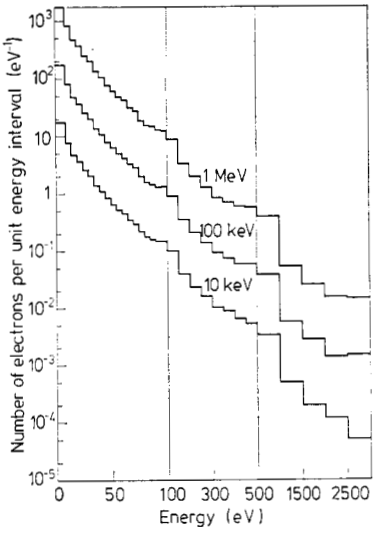

Fig. 4. Number of electrons per unit energy in each of the intervals shown per electron of initial energy 1 MeV, 100 keV and 10 keV. All electrons are degraded to energies below 10 eV. Note the changes in the energy scale at 100 eV and 500 eV.

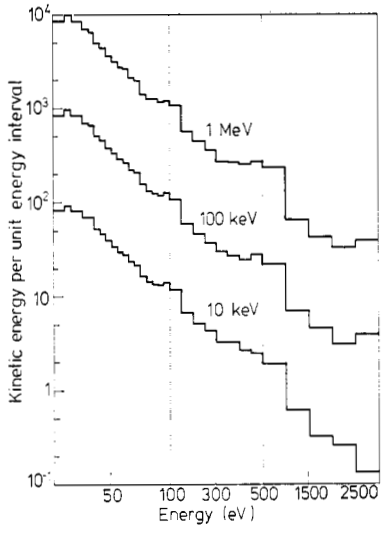

Fig. 5. Kinetic energy of degraded electrons per unit energy interval in each of the intervals shown per incident electron. (The ordinate is dimensionless.) Initial energies are 1 MeV, 100 keV and 10 keV. All electrons are degraded to energies below 10 eV. Note the changes in the energy scale at 100 eV and 500 eV.

each case we find curves which are nearly parallel and separated by decades, corresponding to the differences in initial energies. When compared on the basis of total deposited energy (comparable to normalising to absorbed dose) the curves are very nearly identical. At low dose levels, therefore, one should thus expect spatially correlated events to appear with the same frequency per unit dose at all three incident-electron energies. This conclusion is reinforced by the numerical values, shown in table 1, of the restricted inelastic

Table 1. Restricted inelastic mean free paths

Electron energy (eV)	Mean free path (Å) for an energy transfer greater than				
	10 eV	20 eV	50 eV	100 eV	200 eV
1 000 000	3960	5100	23200	77100	161 000
100 000	1500	1930	8370	27400	58 000
10 000	246	313	1230	3910	8760
4000	115	146	541	1720	4070
2000	65	82	292	934	2350
1000	38	47	159	516	1480
600	26	32	102	342	1300
400	19	24	74	270	—
200	12	15	48	—	—
100	10	13	—	—	—

mean free paths for energy transfer in excess of certain amounts. At energies above several keV, it is unlikely that successive collisions of energy transfer greater than about 50 eV take place within 60 Å of each other (a nominal spacing for DNA strands).

Calculated values of event yields for a number of different end-points in liquid water are shown in table 2 for initial electron energies of 1, 10, 100 and

Table 2. Event yields

	Initial electron energy (keV)			
	1	10	100	1000
Total number of:				
Excitations	26·2	250	2450	24400
Ionisations	31·4	321	3230	32300
Secondaries born above 10 eV	17	155	1520	14800
W-value, eV per ionisation	31·8	31·2	31·0	31·0
G-value, events per 100 eV:				
† H_2O^+	2·45	2·47	2·49	2·49
H^+	0·392	0·404	0·406	0·411
† OH^+	0·274	0·281	0·285	0·286
† O^+	0·027	0·028	0·028	0·029
H_2^+	0·0024	0·0026	0·0025	0·0027
Oxygen K vacancies	—‡	0·0091	0·0109	0·0111

† Excluding oxygen K vacancies.
‡ Not calculated in the present approximation.

1000 keV. As before, all secondary electrons are traced in energy to below 10 eV. Listed are the total number of (non-ionising) excitations and the total number of ionisations of all types, the total number of secondaries above 10 eV, W-values, and G-values for different ionising events. The differences in yields and W-values are remarkably small. (The results are reminiscent of measured W-values for gases determined with incident electron and photon beams over a range of energies.) The W-values remain level as the initial electron energy is decreased down to about 1 keV; it then increases as the initial energy approaches the ionisation potential of the gas.

In the present work we have not been concerned with primary electron energies below 1 keV, but have rather focused attention on higher energies where interpretations of the relative biological effectiveness of different low-LET radiations have seemed to us to be at odds with physical constraints.

The results of Monte Carlo calculations for electrons in the range 30 eV to 20 keV in water have been reported by Paretzke (1975), using cross-sections for water vapour and neglecting K-shell interactions. His results are similar to ours in that the electron slowing-down spectra for 20, 10, 5 and 1 keV primary electrons are congruent at secondary electron energies lower than the primary energy by about a factor of 25, when the spectra are normalised to constant energy input. His W-values are about 3% lower than ours. Paretzke emphasises the biological importance of secondary electrons in the energy range 500 eV to 1–2 keV from low-LET radiations.

4. Discussion

While the present calculations are at the state-of-the-art level and will undoubtedly be revised as better values of the cross-sections become known, we expect only small changes in the relative results obtained. New data could require revision of absolute W-values, yields or the spatial distribution of energy deposition, but relative values of the yields can be expected to remain essentially unchanged.

Our calculations support the validity of the use of absorbed dose as a substantive parameter through which to correlate the effects of low-LET radiations. In the range of electron energies from 1 keV to 1 MeV, end-points that can be attributed to the number or spatial distribution of excitations or ionisations, whether singly or correlated because they come from the same low-energy (less than several keV) electron track, should occur with the same frequency at the same absorbed dose.

While these calculations were made for electrons, the same conclusions apply also to photons. For example, the average kinetic energies of Compton electrons from 1 MeV and 400 keV photons are, respectively, 440 keV and 124 keV (Evans 1958). At lower photon energies the photoelectric effect becomes increasingly important; in the neighbourhood of 50 keV, the initial energy of photoelectrons in water closely approaches the photon energy. Thus gamma rays and X-rays produce electrons with initial energies predominantly in excess of several keV. In the comparison of orthovoltage

($250\ kV_p$) X-rays with ^{60}Co gamma rays, we expect, therefore, that RBE = 1 for effects that arise from the number and distribution of excitations and ionisations at the physical state of the interaction. Substantial differences should not occur even at the lowest energies (about 15 keV) of photons emitted from a beryllium window X-ray tube. This conclusion is in apparent disagreement with that given by Bruce, Pearson and Freedhoff (1963). These authors calculate that the ratio of the number of low-energy ($\lesssim 1$ keV) electrons per rad from gamma and X-rays is about the same (0·8) as the RBE. We will extend our work to include incident photons explicitly and will investigate this point further.

It is from physical end-points such as those calculated here that the chemical reactions leading to the response of the Fricke dosemeter are said to proceed. If, indeed, this is the case, then the yield of the Fricke dosemeter should be independent of the energy of incident electrons or photons from 1 keV to 1 MeV. Experimentally (Shalek and Smith 1969), a gradually accelerating decline in yield is found as the incident energy decreases from 1 MeV to 10 keV, amounting to a total decline of 15% in the G-value. Theoretically, Mozumder and Magee (1966a, b) have found differences in the distribution of low-energy radiation transfer events from primaries of different energies, which may account for the observed differences in chemical yields. For example, they find the ratio of the number of spurs (6 to 100 eV energy transfers) to the number of blobs (100 to 500 eV energy transfers) to be 6·1, 3·9 and 2·5 for primary electrons of energy 1 MeV, 100 keV and 10 keV, respectively. Since our findings may be qualitatively in disagreement with theirs, we plan to recalculate the number of spurs, blobs, short tracks (500 to 5000 eV) and branch tracks (>5000 eV) by their rules in order to make a direct comparison. In essence, Mozumder and Magee do not permit a short track or blob to go on to manufacture additional blobs and spurs, while the present calculations follow all electrons down to 10 eV.

There are substantial differences in the slowing-down spectra at high energies, but these differences tend to disappear at the low-energy ends of the spectra. It is at the low-energy end that the mean free path for energy transfer approximates the separation of DNA strands in biological matter (~ 60 Å). Thus, if cell killing or other biological response is to be attributed to double strand breaks in DNA from the passage of a single electron, there should be no differences in response to different low-LET radiations at all dose levels.

One speaks of target molecular weights of enzyme and virus molecules such that the product of the mass of one molecule and the dose is in the neighbourhood of 65 eV. One then says that 65 eV deposited in the molecule inactivates it. It is more reasonable to think of the inactivation as resulting from the product of electron fluence, ionisation cross-section per atom, and the number of atoms in the molecule. Since dose is proportional to fluence and the number of atoms in the molecules is proportional to molecular weight (for materials of similar composition), the same result is attained. There is the implicit assumption that the molecule acts uniformly and collectively. An ionisation anywhere within it can lead to inactivation.

Typical photographic emulsion grains range in size from about 0·1 to 2 μm. It is the accepted view that an electron passing through an emulsion grain excites internal electrons from the valence to the conduction band of the silver halide crystal. These electrons then migrate to a trapping site where they convert silver ions to silver atoms, forming the latent image. An electron that passes anywhere through the emulsion grain is equally effective. The grain acts uniformly and collectively.

Very little is known about the sensitive sites within the nucleus of a biological cell. We believe that they are associated with the DNA or with the nuclear membrane, perhaps acting in concert. We cannot identify them more clearly; we do not know their size nor whether they act uniformly or collectively.

These considerations are related to microdosimetric studies of the RBE for different low-LET radiations (Kellerer and Rossi 1972, Ellett and Braby 1972, Bond *et al.* 1978). Here the differences in response of biological substances to different radiations are attributed to differences in the spectrum of energy deposition events in sensitive sites ranging in size from 0·5 to 5 μm. The site size in biological substances is determined by fitting predictions from the theory to the measured RBE. These differences in energy deposition events come from differences in the high-energy part of the slowing-down spectrum, especially at energies where the electron range approximates the size of the sensitive site. Thus 5 keV electrons are seen preferentially by a 0·5 μm site, while 50 keV electrons are seen preferentially by a 5 μm site. A theory which emphasises energy deposition events in sites of these sizes thus emphasises the importance of electrons in the 5–50 keV energy region and must, therefore, attribute the biological end-points to other interactions than double strand breaks in DNA from single electrons. There is nothing yet known to suggest that the biological cell mimics photographic emulsion in the size and in the uniform and collective action of its sensitive elements. If, indeed, this is the case, then the microdosimetric model may be valid, and it is the region between 5 and 50 keV in the slowing-down spectrum that is responsible for the observed differences in RBE. A question then remains as to the appropriate dose–response relation for biological sensitive elements, which must form an essential part of any theory of RBE.

Alternatively, if the low-energy electrons are most important in producing the biological end-points of interest, we must question the basis of the observations of differences in response for different low-LET radiations. Here the observed differences cannot be due to the physical stage of the interaction. There are collective effects in water (plasmons) at about 25 eV, but these are preferentially excited by low-energy electrons, say, at 100 eV. We can only speculate that the observed values of the RBE may arise from a difference between the absorbed dose in the tissues or the sensitive sites in the specimen (say, stamen hairs in *Tradescantia*) and the dose measured by the dosemeter. It is possible that there are physiological effects reflecting the differences in penetration of X- and gamma rays. However, the calculations presented here indicate that if the low-energy end of the slowing-down spectrum is of

predominant importance in biological processes, then there is little physical evidence for significantly different RBE values for different low-LET radiations.

This research was sponsored by the Department of Energy under contracts with Union Carbide Corporation and the University of Nebraska.

Résumé

Rendements calculés et spectres de ralentissement des électrons dans l'eau liquide: implications pour RBE photons et électrons

Des calculs Monte Carlo détaillés ont été effectués sur les spectres de ralentissement et les rendements en ce qui concerne un certain nombre de points finals pour des électrons dans de l'eau liquide. Ces enquêtes ont été faites pour étudier des différents effets physiques de différentes radiations à faible LET et différentes implications RBE. Des énergies d'électrons initiales de 1 keV à 1 MeV ont été utilisées et tous les électrons secondaires ont été suivis dans les calculs jusqu'à ce que leur énergie tombe au-dessous de 10 eV. Bien qu'il y ait d'importantes différences quant aux spectres de ralentissement à des énergies proches et supérieures au potentiel d'ionisation de l'oxygène, le spectre d'énergie des électrons à de faibles énergies est essentiellement indépendant de l'énergie initiale de l'électron primaire. Le nombre d'événements par unité d'énergie déposée est aussi essentiellement indépendant de l'énergie d'électrons primaires. Sur la base de ces calculs, il ne semble pas justifier d'attribuer des différences de RBE pour radiations à faible LET à de différents effets physiques produits par des électrons secondaires de faible énergie (environ 1 keV).

Zusammenfassung

Berechnete Resultate und Verlangsamungsspektren für Elektronen in flüssigem Wasser: Folgerungen für die relative biologische Wirksamkeit RBW von Elektronen und Photonen

Detaillierte Monte Carlo-Berechnungen wurden durchgeführt für Verlangsamungsspektren und Resultate für eine Reihe von Elektronen-Endpunkten in flüssigem Wasser. Diese Forschungsarbeiten glaten der Untersuchung der unterschiedlichen physikalischen Auswirkungen unterschiedlicher linearer Energieübertragung bei geringer Bestralung und der Folgerungen für die RBW. Anfänglich wurden Elektronenenergien von 1 keV bis 1 MeV verwendet; alle Sekundärelektronen wurden in den Berechnungen verfolgt, bis ihre Energien unter 10 eV fielen. Obgleich es beträchtliche Unterschiede zwischen den Verlangsamungsspektren bei Energien nahe und über dem K-Hülle Ionisierungspotential von Sauerstoff gibt, hat sich herausgestellt, dass das Energiespektrum von Elektronen bei niedrigeren Energien im wesentlichen unabhängig von der Anfangsenergie des Primärelektrons ist. Die Anzahl der Vorgänge pro Energieeinheit ist ebenfalls im wesentlichen unabhängig von der Energie der Primärelektronen. Diesen Berechnungen zufolge kann man Unterschiede in der RBW bei linearer Energieübertragung mit geringer Bestrahlung praktisch nicht auf die unterschiedlichen physikalischen Effekte durch Sekundärelektronen mit niedriger Energie ($\lesssim 1$ keV) zurückführen.

References

Bermann, F., de Choudens, D., and Descours, S., 1971, in *Advances in Physical and Biological Radiation Detectors* STI/PUB/269 (Vienna: IAEA) p. 311.
Bond, V. P., Meinhold, C. B., and Rossi, H. H., 1978, *Health Phys.*, **34**, 433.
Bruce, W. R., Pearson, M. L., and Freedhoff, H. S., 1963, *Radiat. Res.*, **19**, 606.
Dertinger, H., and Jung, H., 1970, *Molecular Radiation Biology* (New York: Springer Verlag).
Draganic, I. G., and Draganic, Z. D., 1971, *The Radiation Chemistry of Water* (New York: Academic Press).
Dudley, R. A., 1951, *Ph.D. Thesis*, Massachusetts Institute of Technology.
Ellett, W. H., and Braby, L. A., 1972, *Radiat. Res.*, **51**, 229.
Evans, R. D., 1958, in *Encyclopedia of Physics* (Berlin: Springer) vol. 34, p. 266.
Fano, U., and Spencer, L. V., 1975, *Int. J. Radiat. Phys. Chem.*, **7**, 63.
Greening, J. R., 1951, *Proc. Phys. Soc.*, **B64**, 977.

HAMM, R. N., WRIGHT, H. A., RITCHIE, R. H., TURNER, J. E., and TURNER, T. P., 1975, in *Proc. Fifth Symp. on Microdosimetry, Verbania* (Brussels: Euratom) p. 1037.
HELLER, J. M., HAMM, R. N., BIRKHOFF, R. D., and PAINTER, L. R., 1974, *J. Chem. Phys.*, **60**, 3483.
HENDRY, J. H., 1972, *Br. J. Radiol.*, **45**, 923.
ICRU, 1970, *Linear Energy Transfer*, Report 16 (International Commission on Radiation Units and Measurements, P.O. Box 30165, Washington, DC 20014, U.S.A.).
KATZ, R., LARSSON, L., PINKERTON, F. E., and BENTON, E. V., 1977, *Nucl. Track Detection*, **1**, 49.
KATZ, R., and PENNINGTON, E. C., 1978, *Phys. Med. Biol.*, **23**, 1115.
KATZ, R., SHARMA, S. C., and HOMAYOONFAR, M., 1972, *Nucl. Instrum. Meth.*, **110**, 13.
KELLERER, A. M., and ROSSI, H. H., 1972, *Curr. Top. Radiat. Res. Q.*, **8**, 85.
KOBETICH, E. J., and KATZ, R., 1969, *Nucl. Instrum. Meth.*, **71**, 226.
LAW, J., 1969, *Phys. Med. Biol.*, **14**, 607.
LAW, J., 1973, *Phys. Med. Biol.*, **18**, 38.
LAW, J., and NAYLOR, G. P., 1971, *Phys. Med. Biol.*, **16**, 67.
LAW, J., and NAYLOR, G. P., 1972, *Phys. Med. Biol.*, **17**, 400.
LAW, J., and REDPATH, A. T., 1968, *Phys. Med. Biol.*, **13**, 371.
MCLAUGHLIN, M., ROSENSTEIN, M., and LEVINE, H., 1975, in *Biomedical Dosimetry*, STI/PUB/401 (Vienna: IAEA) p. 267.
MOZUMDER, A., and MAGEE, J. L., 1966a, *Radiat. Res.*, **28**, 203.
MOZUMDER, A., and MAGEE, J. L., 1966b, *Radiat. Res.*, **28**, 215.
PALIWAL, B. R., and ALMOND, P. R., 1975, *Phys. Med. Biol.*, **20**, 547.
PARETZKE, H. G., 1975, in *Proc. Fifth Symp. on Microdosimetry, Verbania* (Brussels: Euratom) p. 41.
SCHMID, E., RIMPL, G., and BAUCHINGER, M., 1974, *Radiat. Res.*, **57**, 228.
SHALEK, R. J., and SMITH, C. E., 1969, *Ann. N.Y. Acad. Sci.*, **161**, 44.
SINCLAIR, W. K., and KOHN, H. I., 1964, *Radiology*, **82**, 800.
UNDERBRINK, A. G., KELLERER, A. M., MILLS, R. E., and SPARROW, A. H., 1976, *Radiat. Environ. Biophys.*, **13**, 295.
WAMBERSIE, A., and DUTREIX, A., 1971, in *Biophysical Aspects of Radiation Quality*, STI/PUB/286 (Vienna: IAEA) p. 261.
WAMBERSIE, A., DUTREIX, A., DUTREIX, J., LELLOUCH, J., MOUSTACCHI, E., and TUBIANA, M., 1966, *Int. J. Radiat. Biol.*, **10**, 261.